UC Irvine
UC Irvine Previously Published Works

Title

Vulnerability of the frontal-temporal connections in temporal lobe epilepsy

Permalink

Journal

ISSN

Authors

Lin, Jack J
Riley, Jeffrey D
Juranek, Jenifer
et al.

Publication Date

DOI

Copyright Information

Peer reviewed

Vulnerability of the frontal-temporal connections in temporal lobe epilepsy

Jack J. Lin [a,*], Jeffrey D. Riley [b], Jenifer Juranek [b], Steven C. Cramer [a,b]

[a] *Department of Neurology, University of California, Irvine, Irvine, CA, United States*
[b] *Department of Anatomy and Neurobiology, University of California, Irvine, Irvine, CA, United States*

Summary

Objective: In temporal lobe epilepsy (TLE), frontal-temporal connections are integral parts of the epileptogenic network. Although frontal-temporal gray matter abnormalities have been consistently demonstrated in TLE, white matter connections between these two lobes require further study in this disease setting. We therefore investigated the integrity of two major frontal-temporal white matter association tracts, uncinate fasciculus (UF) and arcuate fasciculus (AF), and their clinical correlates.

Methods: Using diffusion tensor imaging (DTI) tractography, integrity of the UF and AF was examined in 22 individuals (12 subjects with TLE and 10 age-matched healthy controls). DTI indices of these tracts were compared between the two subject groups and correlates examined with clinical variables that included age of seizure onset, duration of epilepsy, history of febrile seizure and antiepileptic medication exposure.

Results: In subjects with TLE, the fractional anisotropy (FA) and apparent diffusion coefficient (ADC) of UF and AF ipsilateral to the side of seizure onset were abnormal when compared to healthy controls. Furthermore, lower UF FA correlated with earlier age of seizure onset.

Conclusion: TLE is associated with abnormal integrity of frontal-temporal white matter tracts, but only on the side of seizure onset. This suggests that frontal-temporal white matter tracts are vulnerable to recurrent seizures and/or the factors precipitating the epilepsy.

© 2008 Elsevier B.V. All rights reserved.

Introduction

Temporal lobe epilepsy (TLE) can have structural and functional effects in distant, discrete brain locations (Bernasconi et al., 2004; Lin et al., 2007; Mueller et al., 2004). The pathophysiology of TLE involves a distributed neuronal network, with intracortical connectivity playing a significant role. In particular, the frontal-temporal association tracts are integral circuits involved in the epileptogenic network

* Corresponding author at: Department of Neurology, University of California Irvine Medical Center, 101 The City Drive S., Building 22C, 2nd Floor, RT 13, Orange, CA 92868, United States.
Tel.: +1 714 456 6203; fax: +1 714 456 6908.
E-mail address: linjj@uci.edu (J.J. Lin).

of TLE. In studies using depth electrodes, the most common route of ictal propagation in TLE is from the temporal lobe toward ipsilateral frontal regions (Lieb et al., 1991; Mayanagi et al., 1996). Interictal hypometabolism seen in positron emission tomography (PET) scans of individuals with TLE often involves not only the temporal lobe but also insular-frontal-opercular regions (Engel et al., 1990; Henry et al., 1993). Furthermore, this pattern of hypometabolism corresponds to ictal EEG discharges and seizure propagation pathways (Chassoux et al., 2004). Frontal-temporal white matter association tracts thus play a critical role in seizure propagation in TLE.

These findings suggest that frontal-temporal white matter association tracts might become compromised as part of the TLE disease process. The current study addressed the hypothesis that the integrity of frontal-temporal white matter connections is reduced in subjects with TLE, specifically on the side of seizure onset. To this end, we investigated two major frontal-temporal association tracts, uncinate fasciculus (UF) and arcuate fasciculus (AF), in subjects with TLE and in healthy controls. We also considered how the integrity of these two tracts relates to a number of clinical variables that might theoretically correlate with TLE-associated white matter tract abnormalities.

The method used to examine white matter integrity was diffusion tensor imaging (DTI), a magnetic resonance imaging technique that measures water diffusion and its directionality in three-dimensions, and is thus uniquely suited to address study hypotheses (Basser and Pierpaoli, 1996). The primary DTI endpoint used to address the hypothesis was fractional anisotropy (FA), which characterizes the degree to which diffusion is directional. Normal white matter tracts have highly directional diffusion (high FA), whereas degenerated tracts have reduced directional diffusion (low FA) (Basser and Pierpaoli, 1996). Other measures of white matter integrity derived from DTI, including apparent diffusion coefficient, perpendicular and parallel diffusivity, were also examined as secondary endpoints.

Methods

Subjects

A total of 12 patients with TLE (age = 37.9 ± 3.2 years, mean $\pm$ S.E.M., range: 20–52; female/male = 9/3) and 10 age-matched healthy controls (42.1 ± 3.1 years, range: 33–55; female/male = 4/6) were recruited. Entry criteria for patients included ability to undergo MRI, plus definite or probable unilateral TLE. The diagnosis of TLE was based on clinical history, seizure semiology, and ictal or interictal electroencephalography (EEG) criteria. A total of 11 patients had continuous video-EEG monitoring, demonstrating spontaneous seizures with unilateral temporal lobe onset and thus were classified as *definite* TLE. Only one patient did not undergo ictal EEG recording but had predominately left temporal interictal epileptiform discharges with appropriate seizure semiologies described by the patient and his/her family and thus were classified as *probable* left TLE. Age of seizure onset was defined as the age when a patient began having recurrent unprovoked seizures. Seizure frequency and antiepileptic medication history were obtained from detailed chart review and patient interviews. Detailed clinical characteristics of the 12 TLE patients are outlined in Table 1.

The control subjects were recruited through responses to flyer advertisements posted at the University of California, Irvine (UC Irvine) Medical Center and School of Medicine. Criteria for controls subjects included (1) no history of seizures or seizure-like attacks or a neurological disorder, (2) no family member with epilepsy, (3) no history of a loss of consciousness for >5 min, and (4) ability to undergo MRI. This study was approved by the Institutional Review Board at UC Irvine.

MRI acquisition

MR data were acquired with a 3-T MR scanner (Siemens Trio, Erlangen, Germany) with an 8 phased array head coil. DTI data were acquired using a single-shot echo-planar pulse sequence with parallel acquisition technique (IPAT) in conjunction with generalized autocalibrating partially parallel acquisition (GRAPPA). The image matrix was 128×128, with a 256 mm × 256 mm field of view, TR = 9300 ms, TE = 93 ms. Axial slices of 2.0 mm were acquired with no interslice gap. Diffusion gradients were applied in 12 non-collinear directions with a *b* value of 1000 s/mm. To enhance signal to noise ratio, we repeated the image two times. Acquisition time for the entire data set was approximately 7 min. For anatomical guidance, a 3D magnetization-prepared, rapid-acquisition, gradient-echo images (MP-RAGE) image set with 1 mm isotropic voxels was obtained using TR = 1620 ms, TE = 3.87 ms, and flip angle 15°.

Image analysis

3D fiber tracking reconstruction was performed using DTI Studio software (H. Jiang and S. Mori; Johns Hopkins University, Baltimore, MD; http://cmrm.med.jhmi.edu/), which uses fiber assignment by means of continuous fiber tracking (12). All DTI raw data images were first visually inspected in a slice-wise manner by a single author (JDR) and images with visually apparent bulk motion artifacts were removed (13). Parallel acquisition techniques employed in this study have significantly reduced motion and thus co-registration was not performed. Our DTI images set had low eddy current related geometric distortion geometric distortion between images obtained in each motion-probing gradient direction and thus eddy current correction was not applied for this data set (Bastin and Armitage, 2000; Naganawa et al., 2004). Computational analyses of diffusion weighted magnetic resonance images then enabled formation of a diffusion tensor, which describes the degree and direction of diffusion for each voxel of brain scanned. This allows for the construction of white matter tracts and the calculation of three eigenvalues, corresponding to eigenvectors oriented along three orthogonal directions (λ_1, λ_2 and λ_3). The largest diffusion direction (λ_1) represents diffusivity parallel to the principal axis of the axonal fibers ($\lambda_{||}$), whereas diffusivity perpendicular to the axon fibers, $\lambda_{\perp}$, is expressed as $(\lambda_2 + \lambda_3)/2$. Fibers are tracked along the principle eigenvector ($\lambda_{||}$) until the FA decreases below a preset threshold of 0.20. To avoid fibers with sharp turns and therefore minimize the erroneous inclusion of fibers not belonging to the tract of interest, fiber tracking is discontinued when angles greater than 80° are encountered.

Based on the anatomy of the UF, two rectangular regions of interest (ROIs) were used to reconstruct this tract, each measuring approximately 50 voxels (14, 15) (Fig. 1). One ROI was placed in the axial plane just as the UF begins to travel ventrally in the temporal stem via the external and extreme capsules, at or near the level of the anterior commissure. The second ROI was placed in the axial plane at the ventral end of the temporal lobe, just dorsal to where the fibers run into the middle temporal gyrus. For the AF, three ROIs were required to adequately reconstruct this tract, two rectangular regions measuring approximately 50 voxels and one triangular region measuring approximately 25 voxels (Fig. 2). One rectangular

Table 1 Summary of temporal lobe epilepsy patient clinical characteristics

| Patient	Age (years)	Seizure onset age (years)	Duration of epilepsy	Initial precipitating factor	Seizure frequency (per month)	MRI (clinical)	EEG	PET	Antiepileptic medications (current and past*)
1	34	19	15	None	1	Right temporal lobar atrophy	Right temporal	Right temporal hypometabolism	PHT, LEV
2	52	1	51	Febrile seizure	2	Left MTS	Left temporal	Normal	CBZ, LEV, LTB, PHT*, PB*, PRM*, TPM*
3	45	36	9	Head trauma	3	Normal	Left temporal	Left temporal hypometabolism	OXC, VPA, LEV*, TPM*
4	49	12	37	None	0.5	Right MTS	Right temporal	Right temporal hypometabolism	LEV, LGT, PHT*, PB*, CBZ*, PB*, GBP*
5	39	21	18	None	1	Normal	Left ≫ right interictal temporal sharp waves	—	LGT, LEV*
6	28	2	26	Febrile seizure	0.5	Normal	Left temporal	Normal	CBZ, LGT, PB*, FBM*, ZNS*, OXC*
7	50	39	11	None	2	Left MTS	Left temporal	Left temporal hypometabolism	PHT, TPM, LGT*, LEV*
8	33	7	26	None	8	Left MTS	Left temporal	Left temporal hypometabolism	CBZ, LEV, PHT, TPM
9	20	8	12	None	3	Normal	Left temporal	Left temporal hypometabolism	LGT, PB*, CBZ*, PHT*
10	24	11	13	Head trauma	6	Normal	Left temporal	Normal	LEV, OXC, CBZ*, GBP*
11	37	12	25	Febrile seizure	2	Normal	Left temporal	Normal	LEV, OXC
12	34	4	30	Febrile seizure	8	Left MTS	Left temporal	Left temporal hypometabolism	PHT, GBP, LEV

MRI = magnetic resonance imaging; EEG = electroencephalogram; PET = positron emissions tomography; MTS = mesial temporal sclerosis; PHT = phenytion; LEV = levetiracetam; CBZ = carbamazepine; LGT = lamotrigine; PB = phenobarbital; PRM = primidone; TPM = topiramate; OXC = oxcarbazepine; VPA = valproic acid; GBP = gabapentin; FBM = felbamate; ZNS = zonisamide; — indicates test not done.
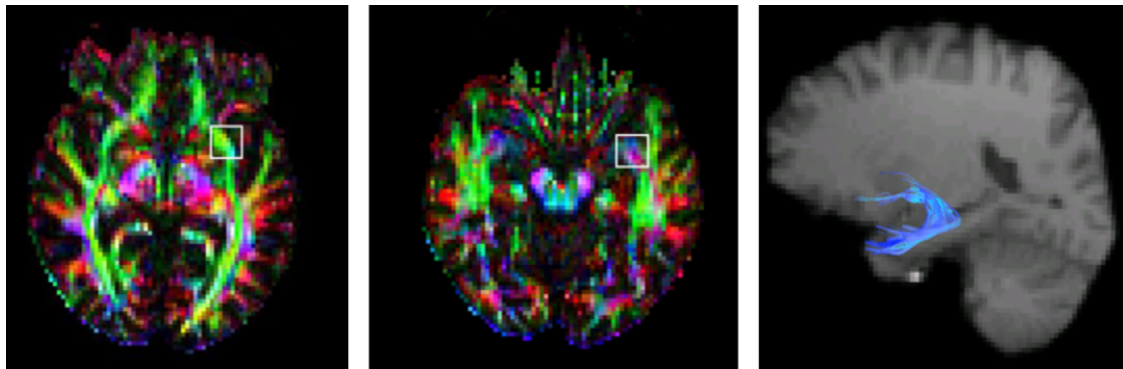
Figure 1 Region of interest (ROI) placement for tract selection of the uncinate fasciculus. Colored-coded maps were used to represent tract information, with red, green, and blue colors denoted as right—left, anterior—posterior, and superior—inferior orientations, respectively. The first ROI was placed in the axial plane just as the uncinate fasciculus begins to travel ventrally in the temporal stem via the external and extreme capsules (A). The second ROI was placed in the axial plane at the ventral end of the temporal lobe, just dorsal to where the fibers run into the middle temporal gyrus (B). Illustrative color figure displaying the diffusion tensor reconstructed fiber tract of the uncinate fasciculus, overlaid on a sagittal T1 image (C).

ROI was placed in the coronal plane in the region where AF travels lateral to the corticospinal tract. The second rectangular ROI was placed in the coronal plane at the rostral surface of the splenium, in the region of the AF. The third triangular ROI was placed in the axial plane, in the region where the AF travels ventrally in the posterior parietal lobe. In a few instances, tract generation yielded fibers that are clearly not part of the tract of interest (''non-anatomical'') and were therefore manually removed. This was done by creating whole-slice exclusionary ROIs using the 'not' function provided by DTI Studio. For the UF, these ROIs were placed in the mid-sagittal plane when stray fibers crossed the midline, as well as in the coronal plane when stray fibers continued to travel posterior to the
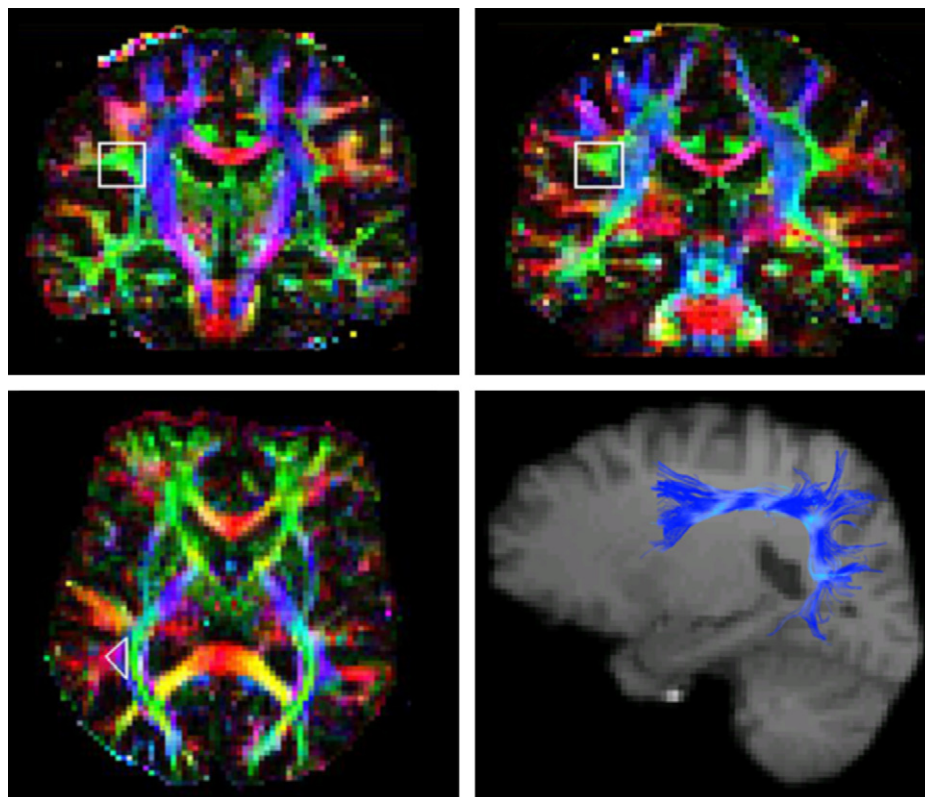
Figure 2 Region of interest (ROI) placement for tract selection of the arcuate fasciculus. Same color-coded maps were used as Fig. 1 to represent fiber orientation. The first ROI was placed in the coronal plane in the region where arcuate fasciculus travels lateral to the corticospinal tract (A). The second ROI was placed in the coronal plane at the rostral surface of the splenium (B). The third ROI was placed in the axial plane, in the region where the arcuate fasciculus travels ventrally in the posterior parietal lobe (C). Illustrative figure showing the diffusion tensor reconstructed fiber tract of arcuate fasciculus overlaid on a sagittal B0 image (D).

temporal stem (fibers that did not curve back toward the frontal lobe). For the AF, these ROIs were restricted to the mid-sagittal slice for those fibers that crossed the midline. Statistical software included in DTI Studio was then used to determine the integrity of the generated tract (12, 13, 16). Measures of integrity included the mean fractional anisotropy (FA), which assesses the degree to which diffusion is directional; apparent diffusion coefficient, a measure

of mean diffusivity; parallel diffusivity ($\lambda_{||}$), the predominant direction of diffusion; and perpendicular diffusivity ($\lambda_{\perp}$).

Statistical analysis

Wilcoxon signed rank test was performed to compare the FA values ipsilateral and contralateral to the side of seizure onset. The

**Table 2** Comparisons between DTI values of temporal lobe epilepsy patients and control subjects

	Ipsi	Contra	Control	Ipsi vs. control	Contra vs. control	Ipsi vs. contra
UF FA	0.362 ± 0.007	0.391 ± 0.007	0.40 ± 0.01	$p < 0.005$	NS	$p < 0.015$
UF ADC	2.791 ± 0.038	2.650 ± 0.023	2.615 ± 0.042	$p < 0.01$	NS	$p < 0.015$
UF perpendicular diffusivity	0.750 ± 0.014	0.688 ± 0.009	0.673 ± 0.016	$p < 0.004$	NS	$p < 0.002$
UF parallel diffusivity	1.292 ± 0.023	1.292 ± 0.015	1.285 ± 0.024	NS	NS	NS
AF FA	0.446 ± 0.005	0.453 ± 0.006	0.471 ± 0.007	$p < 0.012$	NS	NS
AF ADC	2.367 ± 0.014	2.312 ± 0.083	2.285 ± 0.022	$p < 0.01$	NS	NS
AF perpendicular diffusivity	0.577 ± 0.006	0.571 ± 0.009	0.558 ± 0.010	NS	NS	NS
AF parallel diffusivity	1.192 ± 0.008	1.167 ± 0.014	1.190 ± 0.010	NS	NS	NS

DTI = diffusion tensor imaging; UF = uncinate fasciculus; AF = arcuate fasciculus; FA = fractional anisotropy; ADC = apparent diffusion coefficient; Ipsi = ipsilateral to the side of seizure onset; Contra = contralateral to the side of seizure onset; NS = not significant; units for ADC, perpendicular and parallel diffusivity = $\times 10^{-3}$ mm^2/s.

Uncinate Fasciculus
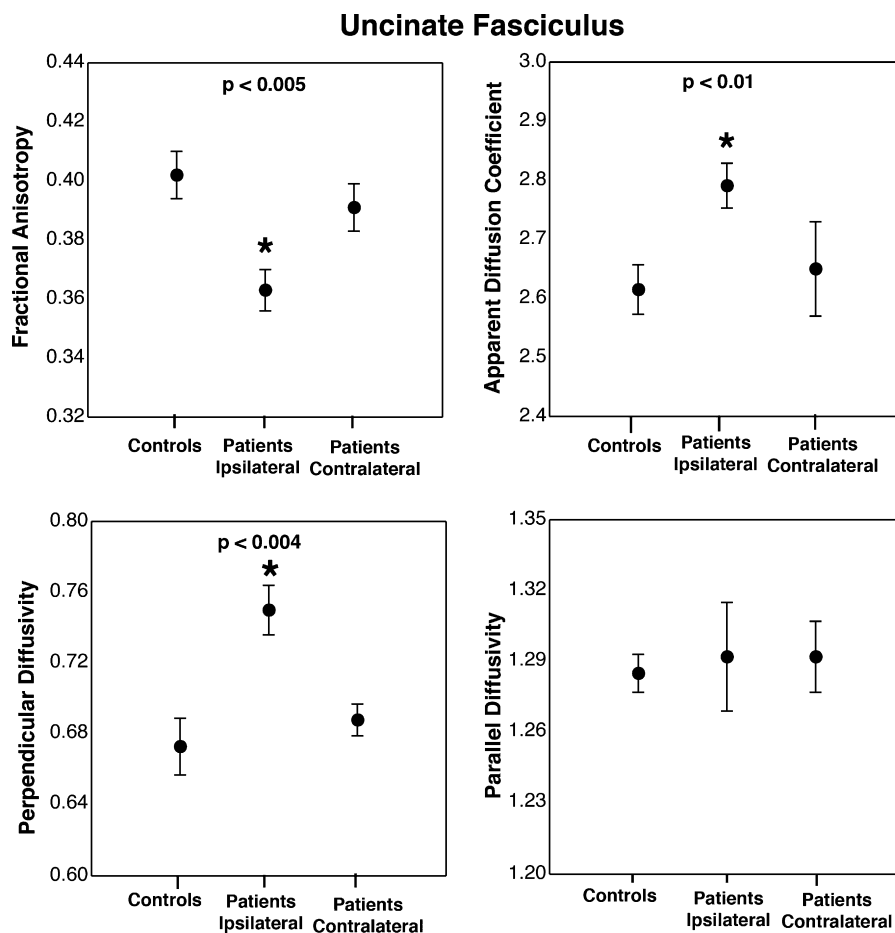
Figure 3 Diffusion tensor imaging measurements in the uncinate fasciculus of control and TLE subjects ipsilateral and contralateral to the seizure focus. Significant differences (*p* value denoted in the graph) between controls and TLE subjects ipsilateral to the seizure focus are indicated with *. The unit for apparent diffusion coefficient, parallel and perpendicular diffusivity is 10^{-3} mm^2/s.

Arcuate Fasciculus
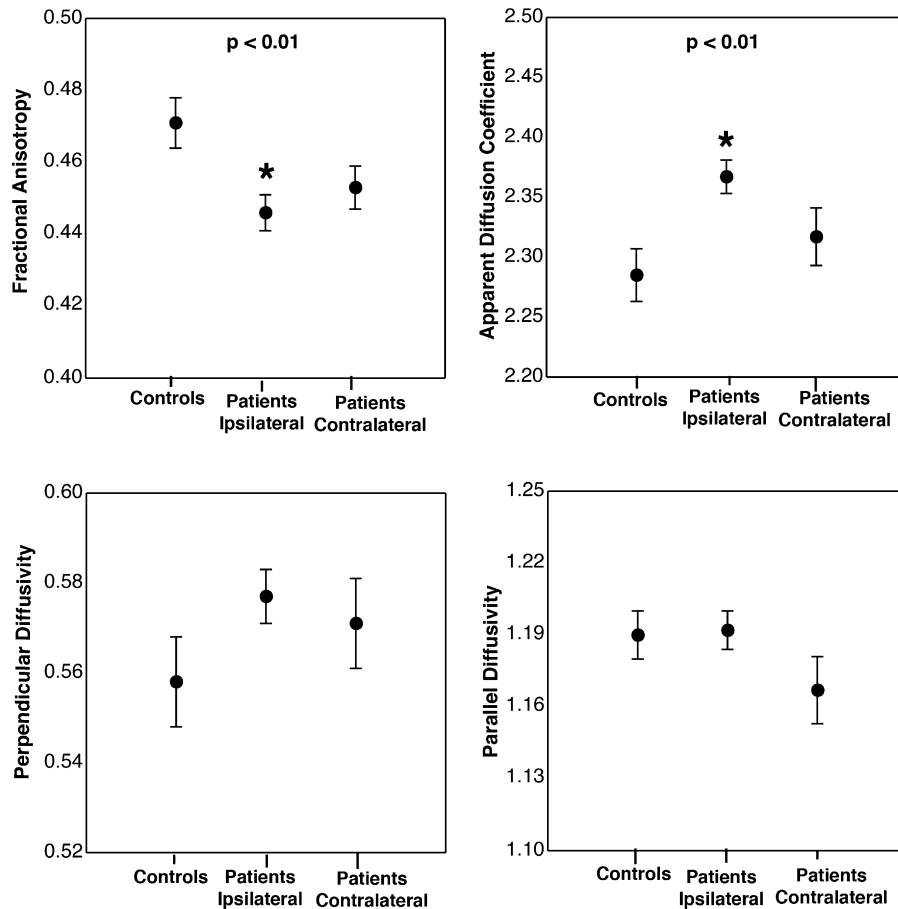
Figure 4 Diffusion tensor imaging measurements in the arcuate fasciculus of control and TLE subjects ipsilateral and contralateral to the seizure focus. Significant differences (p value denoted in the graph) between controls and TLE subjects ipsilateral to the seizure focus are indicated with *. The unit for apparent diffusion coefficient, parallel and perpendicular diffusivity is 10^{-3} mm^2/s.

Wilcoxon rank-sum test was used to compare DTI values between TLE and healthy controls. To account for multiple comparisons (Table 2), we used the Bonferroni correction and considered significant only those DTI values for which $p < 0.05/3 = 0.017$. Spearman's Rho was used to assess the relationship between DTI measurements and clinical variables.

Interrater reliability

To evaluate interrater reliabilities for the fiber tracts generated, 10 brains were randomly chosen (5 TLE and 5 healthy control). Working independently but using the same DTI protocol, the two raters generated the UF FA values. There was a high interrater reliability for the UF FA with intraclass correlation coefficient (ICC) measured at 0.85 for right UF and 0.80 for left UF.

Results

TLE patients have abnormal frontal-temporal connections only ipsilateral to the side of seizure onset

The two major frontal-temporal tracts, UF and AF, both ipsilateral and contralateral to the side of seizure onset,

were compared among the TLE patients as well as to the healthy control subjects. For control subjects, there was no significant right–left asymmetry in FA values: (left UF FA = 0.41 ± 0.01 vs. right UF FA = 0.39 ± 0.01, $p = 0.22$; left AF FA = 0.47 ± 0.01 vs. right AF FA 0.47 ± 0.01, $p = 0.80$). Therefore, the mean right and left values for FA values was used when for comparisons with data from subjects with TLE. The results are presented in Table 2.

Both UF and AF FA ipsilateral to the side of seizure onset were significantly lower when compared to control values. On the other hand, no significant difference was found when comparing the FA values contralateral to the side of seizure onset with control (Figs. 3 and 4). Among subjects with TLE, FA ipsilateral to the side of seizure onset was lower than FA contralateral, significantly so for UF.

Other DTI changes

Compared to healthy controls, both UF and AF apparent diffusion coefficients (ADC) were elevated in the TLE patients ipsilateral to the side of seizure onset. Perpendicular diffusivity in UF ipsilateral to the side of seizure focus was also increased in the TLE group as compared to healthy controls.
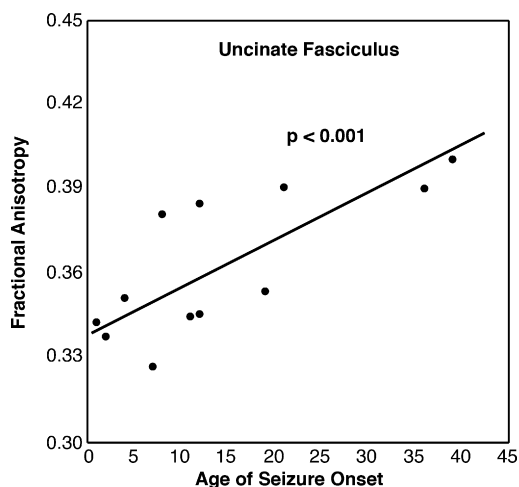
Figure 5 Age of seizure onset correlated with uncinate fasciculus integrity as measure by fractional anisotropy (FA). The scatter graph shows a linear correlation between age of seizure onset and FA. Highly significant linkage was found relating earlier age of seizure onset with lower FA in the ipsilateral uncinate fasciculus ($r = 0.83$, $p < 0.001$).

No significant differences in parallel diffusivity for the ipsilateral UF were found between groups (Fig. 3). Contrary to the findings of UF, the increased in ADC found in AF was not accompanied by an increase in perpendicular or parallel diffusivity (Fig. 4). In all cases, no significant differences in DTI measures were seen when the side contralateral to seizure onset was compared to results in healthy controls.

Changes in uncinate fasciculus integrity are related to age of seizure onset

Earlier age of seizure onset correlated with reduced UF FA ipsilateral, but not contralateral, to seizure focus (Fig. 5, $r = 0.83$, $p < 0.001$). Similarly, a correlation between longer duration of epilepsy and elevated UF ADC ipsilateral to seizure focus showed a trend ($r = 0.57$, $p = 0.052$). No relationship was found between AF FA and age of seizure onset or duration of epilepsy. Further, the FA values of either frontal-temporal tract did not correlate with seizure frequency, febrile seizures or antiepileptic medication history.

Discussion

The current study aimed to better understand propagation of TLE effects across a distributed neuronal network. Using DTI, the integrity of two frontal-temporal white matter tracts was assessed. The major findings of this study are (1) as compared to healthy age-matched controls, TLE is associated with altered frontal-temporal connections, specifically on the side of seizure onset, and (2) this finding is most pronounced in subjects with earlier age of seizure onset, at least in one of the two tracts examined (UF).

There is convergent evidence that TLE has structural and functional abnormalities that extend beyond the epileptogenic temporal lobe. Morphometric brain imaging techniques such as voxel base morphometry (VBM) and cortical sulcal matching have consistently shown decreased bilateral gray matter density or thickness in the temporal and frontal lobes (Bernasconi et al., 2004; Bonilha et al., 2006; Keller et al., 2004; Lin et al., 2007). These studies often postulate that the distributed gray matter abnormalities in the frontal and temporal lobes are due to a widespread epileptogenic network in TLE. However, the observed extratemporal gray matter abnormalities are not specific to the side of seizure focus. In contrast, voxel-based statistics parametric mapping (SPM) methods applied to MR T2 relaxometry have yielded asymmetric distribution of abnormalities preferentially ipsilateral to the seizure focus (Pell et al., 2004; Rugg-Gunn et al., 2005). Mueller and colleagues found mesial temporal lobe epilepsy subjects have most severe T2 relaxation reduction not only in the ipsilateral hippocampus but also ipsilateral neocortical temporal lobe, orbitofrontal and parietal regions (Mueller et al., 2007). A lesser degree of T2 relaxation rate decrease was also found in the contralateral frontal lobe. In a composite voxel-based analysis of white matter volume and T2 relaxometry, Pell and colleagues found left temporal lobe epilepsy patient has the largest cluster of T2 abnormality in the left mesial and lateral temporal lobe and this region overlaps with white matter volume reduction (Pell et al., 2008). Whole brain MR diffusion abnormalities and their relationship to epileptogenic zone have also been explored with VBM. Thivard and investigators showed 7 out of 16 patients had diffusion abnormalities that concurred with intracranial stereo-electroencephalography (SEEG) defined irritative zone (Thivard et al., 2006).

Although voxel-based analyses help elucidate extratemporal structural abnormalities in TLE, they do not provide measures of frontal-temporal white matter integrity. DTI provides connectivity data, and thus provides insights on white matter integrity of specific tracts. In our current study, we investigated two major frontal-temporal association pathways, UF and AF. The UF connects the superior temporal gyrus to the orbital and frontal polar regions, while the AF connects the superior temporal gyrus to the perisylvian frontal-parietal cortex (Ebeling and von Cramon, 1992; Catani et al., 2002; Makris et al., 2005) (see Figs. 1 and 2). We found decreased DTI indices of tract integrity in both of these association pathways ipsilateral, but not contralateral, to the side of seizure onset. Our results are consistent with Rodrigo and colleagues who found that the right UF FA is reduced in patients with right TLE when compared to healthy controls, although these authors did not study TLE of left brain origin, nor did they correlate FA measures with clinical variables (Rodrigo et al., 2007). The current study included patients with both right and left TLE, although majority of our patients had left TLE. In addition, investigation of a second frontal-temporal tract, the AF, confirmed the lateralized diffusion abnormalities (Fig. 3). The fact that reduced FA in both tracts is isolated to the side seizure focus in our study provides additional support for frontal-temporal tract involvement in the epileptogenic network of TLE.

The pathophysiological mechanisms underlying the FA reduction and ADC elevation in these two tracts may be different based on their distinct directional diffusion characteristics. In animal studies, myelin degeneration is characterized by decrease FA, increased diffusivity perpendicular to the axon bundle and relative preservation of

parallel diffusivity (Gulani et al., 2001; Song et al., 2003, 2005). This is precisely the pattern of DTI change found in UF, suggesting the alteration in white matter integrity in this tract is due a structural abnormality such as myelin derangement. However, in AF, the FA reduction and ADC elevation are not associated with abnormal directional diffusivity. Elevated ADC has been associated with vasogenic edema secondary to increased interstitial fluid (Gass et al., 2001; Kuroiwa et al., 1999). The patients in this study had medically intractable epilepsy and the ongoing seizures may result in interstitial edema in AF.

The association between earlier seizure onset and reduced FA in UF is an interesting finding that requires further study. UF as well as other white matter tracts undergo significant age-related changes in normal brain development (Mukherjee et al., 2001, 2002; Eluvathingal et al., 2007). However, the effect of epilepsy, or factors precipitating epilepsy, on the integrity of these white mater tracts during brain maturation remains unexplored. The current finding that earlier age of seizure onset is associated with greater derangement of UF integrity suggests that such an effect might exist. Immature brain maybe more vulnerable to age related white matter tract changes. To test this hypothesis, our next study will prospectively compute the developmental trajectory of white matter tracts in children with new onset epilepsy, relative to healthy controls, and correlate these differences with the age of seizure onset.

Brain abnormalities in subjects with TLE extend beyond the seizure focus. The current study documents changes in white matter tracts and their relationship to age of seizure onset and duration of epilepsy. These findings provide insights into the pathophysiology of TLE.

Conflict of interest

The authors report no conflict of interest.

Acknowledgments

References

Basser, P.J., Pierpaoli, C., 1996. Microstructural and physiological features of tissues elucidated by quantitative-diffusion-tensor MRI. J. Magn. Reson. B 111, 209—219.

Bastin, M.E., Armitage, P.A., 2000. On the use of water phantom images to calibrate and correct eddy current induced artefacts in MR diffusion tensor imaging. Magn. Reson. Imaging 18, 681—687.

Bernasconi, N., Duchesne, S., Janke, A., Lerch, J., Collins, D.L., Bernasconi, A., 2004. Whole-brain voxel-based statistical analysis of gray matter and white matter in temporal lobe epilepsy. Neuroimage 23, 717—723.

Bonilha, L., Rorden, C., Appenzeller, S., Carolina Coan, A., Cendes, F., Min Li, L., 2006. Gray matter atrophy associated with duration of temporal lobe epilepsy. Neuroimage 32 (3), 1070—1079.

Catani, M., Howard, R.J., Pajevic, S., Jones, D.K., 2002. Virtual in vivo interactive dissection of white matter fasciculi in the human brain. Neuroimage 17, 77—94.

Chassoux, F., Semah, F., Bouilleret, V., Landre, E., Devaux, B., Turak, B., Nataf, F., Roux, F.X., 2004. Metabolic changes and electro-clinical patterns in mesio-temporal lobe epilepsy: a correlative study. Brain 127, 164—174.

Ebeling, U., von Cramon, D., 1992. Topography of the uncinate fascicle and adjacent temporal fiber tracts. Acta Neurochir. (Wien) 115, 143—148.

Eluvathingal, T.J., Hasan, K.M., Kramer, L., Fletcher, J.M., Ewing-Cobbs, L., 2007. Quantitative diffusion tensor tractography of association and projection fibers in normally developing children and adolescents. Cereb. Cortex 17, 2760—2768.

Engel Jr., J., Henry, T.R., Risinger, M.W., Mazziotta, J.C., Sutherling, W.W., Levesque, M.F., Phelps, M.E., 1990. Presurgical evaluation for partial epilepsy: relative contributions of chronic depth-electrode recordings versus FDG-PET and scalp-sphenoidal ictal EEG. Neurology 40, 1670—1677.

Gass, A., Niendorf, T., Hirsch, J.G., 2001. Acute and chronic changes of the apparent diffusion coefficient in neurological disorders—biophysical mechanisms and possible underlying histopathology. J. Neurol. Sci. 186 (Suppl. 1), S15—S23.

Gulani, V., Webb, A.G., Duncan, I.D., Lauterbur, P.C., 2001. Apparent diffusion tensor measurements in myelin-deficient rat spinal cords. Magn. Reson. Med. 45, 191—195.

Henry, T.R., Mazziotta, J.C., Engel Jr., J., 1993. Interictal metabolic anatomy of mesial temporal lobe epilepsy. Arch. Neurol. 50, 582—589.

Keller, S.S., Wilke, M., Wieshmann, U.C., Sluming, V.A., Roberts, N., 2004. Comparison of standard and optimized voxel-based morphometry for analysis of brain changes associated with temporal lobe epilepsy. Neuroimage 23, 860—868.

Kuroiwa, T., Nagaoka, T., Ueki, M., Yamada, I., Miyasaka, N., Akimoto, H., Ichinose, S., Okeda, R., Hirakawa, K., 1999. Correlations between the apparent diffusion coefficient, water content, and ultrastructure after induction of vasogenic brain edema in cats. J. Neurosurg. 90, 499—503.

Lieb, J.P., Dasheiff, R.M., Engel Jr., J., 1991. Role of the frontal lobes in the propagation of mesial temporal lobe seizures. Epilepsia 32, 822—837.

Lin, J.J., Salamon, N., Lee, A.D., Dutton, R.A., Geaga, J.A., Hayashi, K.M., Luders, E., Toga, A.W., Engel Jr., J., Thompson, P.M., 2007. Reduced neocortical thickness and complexity mapped in mesial temporal lobe epilepsy with hippocampal sclerosis. Cereb. Cortex 17, 2007—2018.

Makris, N., Kennedy, D.N., McInerney, S., Sorensen, A.G., Wang, R., Caviness Jr., V.S., Pandya, D.N., 2005. Segmentation of subcomponents within the superior longitudinal fascicle in humans: a quantitative, in vivo, DT-MRI study. Cereb. Cortex 15, 854—869.

Mayanagi, Y., Watanabe, E., Kaneko, Y., 1996. Mesial temporal lobe epilepsy: clinical features and seizure mechanism. Epilepsia 37 (Suppl. 3), 57—60.

Mueller, S.G., Laxer, K.D., Cashdollar, N., Flenniken, D.L., Matson, G.B., Weiner, M.W., 2004. Identification of abnormal neuronal metabolism outside the seizure focus in temporal lobe epilepsy. Epilepsia 45, 355—366.

Mueller, S.G., Laxer, K.D., Schuff, N., Weiner, M.W., 2007. Voxel-based T2 relaxation rate measurements in temporal lobe epilepsy (TLE) with and without mesial temporal sclerosis. Epilepsia 48, 220—228.

Mukherjee, P., Miller, J.H., Shimony, J.S., Conturo, T.E., Lee, B.C., Almli, C.R., McKinstry, R.C., 2001. Normal brain matura-

tion during childhood: developmental trends characterized with diffusion-tensor MR imaging. Radiology 221, 349—358.

Mukherjee, P., Miller, J.H., Shimony, J.S., Philip, J.V., Nehra, D., Snyder, A.Z., Conturo, T.E., Neil, J.J., McKinstry, R.C., 2002. Diffusion-tensor MR imaging of gray and white matter development during normal human brain maturation. AJNR Am. J. Neuroradiol. 23, 1445—1456.

Naganawa, S., Koshikawa, T., Kawai, H., Fukatsu, H., Ishigaki, T., Maruyama, K., Takizawa, O., 2004. Optimization of diffusion-tensor MR imaging data acquisition parameters for brain fiber tracking using parallel imaging at 3 T. Eur. Radiol. 14, 234—238.

Pell, G.S., Briellmann, R.S., Pardoe, H., Abbott, D.F., Jackson, G.D., 2008. Composite voxel-based analysis of volume and T2 relaxometry in temporal lobe epilepsy. Neuroimage 39, 1151—1161.

Pell, G.S., Briellmann, R.S., Waites, A.B., Abbott, D.F., Jackson, G.D., 2004. Voxel-based relaxometry: a new approach for analysis of T2 relaxometry changes in epilepsy. Neuroimage 21, 707—713.

Rodrigo, S., Oppenheim, C., Chassoux, F., Golestani, N., Cointepas, Y., Poupon, C., Semah, F., Mangin, J.F., Le Bihan, D., Meder, J.F.,

2007. Uncinate fasciculus fiber tracking in mesial temporal lobe epilepsy. Initial findings. Eur. Radiol. 17, 1663—1668.

Rugg-Gunn, F.J., Boulby, P.A., Symms, M.R., Barker, G.J., Duncan, J.S., 2005. Whole-brain T2 mapping demonstrates occult abnormalities in focal epilepsy. Neurology 64, 318—325.

Song, S.K., Sun, S.W., Ju, W.K., Lin, S.J., Cross, A.H., Neufeld, A.H., 2003. Diffusion tensor imaging detects and differentiates axon and myelin degeneration in mouse optic nerve after retinal ischemia. Neuroimage 20, 1714—1722.

Song, S.K., Yoshino, J., Le, T.Q., Lin, S.J., Sun, S.W., Cross, A.H., Armstrong, R.C., 2005. Demyelination increases radial diffusivity in corpus callosum of mouse brain. Neuroimage 26, 132—140.

Thivard, L., Adam, C., Hasboun, D., Clemenceau, S., Dezamis, E., Lehericy, S., Dormont, D., Chiras, J., Baulac, M., Dupont, S., 2006. Interictal diffusion MRI in partial epilepsies explored with intracerebral electrodes. Brain 129, 375—385.